

EXPERIMENTAL STUDIES OF RATE-DEPENDENT MECHANICAL BEHAVIOR OF LAMINATED RUBBER BEARINGS

T. Imai¹, A.R. Bhuiyan², M. K. Razzaq³, Y. Okui³, and H. Mitamura⁴

¹ Rubber Bearing Association, Japan

² Department of Civil Engineering, Chittagong University of Engineering and Technology, Bangladesh

³ Department of Environmental Science and Civil Engineering, Saitama University, Japan

⁴ Civil Engineering Research Institute for Cold Region, PWRI, Japan

Abstract: The paper is devoted towards an experimental investigation of the rate-dependent mechanical behavior of the laminated rubber bearings under horizontal shear deformation with a constant vertical compressive load. Three types of bearings are used in this study: natural rubber bearings (RBs), lead rubber bearings (LRBs) and high damping rubber bearings (HDRBs) with ISO standard geometry. The experimental scheme is comprised of three types of test at room temperature (23 ± 1 °C): cyclic shear (CS) test, multi-step relaxation (MSR) test, and simple relaxation (SR) test. The purpose of conducting the CS test is to identify the instantaneous behavior of the bearings; the SR test, to evaluate the viscosity induced rate-dependent behavior; and finally the MSR test, to obtain the equilibrium behavior. Moreover, a series of sinusoidal loading tests (at 0.5 Hz) are carried out at different temperatures ranging from 23°C to -30 °C. The objective of conducting the sinusoidal loading tests is to identify the basic mechanical characteristics of the bearings at different temperatures: the equivalent stiffness and damping of the bearings. The experimental results show that the viscosity induced rate-dependent behavior is more prominent in the HDR than the LRB and the RB. The viscosity induced rate-dependent behavior of the bearings is more significantly appeared in loading than in unloading. However, this typical behavior is not so significant in the RB as in the other two bearings. Furthermore, the temperature dependency of the equivalent stiffness is more remarkably emerged in the HDR and RB than the LRB, while that of the equivalent damping is more significant in the RB than the others.

1. INTRODUCTION

An isolation bearing is able to provide a structure with additional horizontal flexibility and energy dissipation. Three types of laminated rubber bearings are usually used in highway bridges for this purpose: natural rubber bearings (RBs), lead rubber bearings (LRBs) and high damping rubber bearings (HDRBs).

Several authors have conducted different loading experiments on laminated rubber bearings in order to acquire deep understanding of the mechanical properties. The work of Abe et al. (2004); Aiken et al. (1992); Kikuchi and Aiken (1997); Sano and D Pasquale (1995) can be noted. They have applied uni-directional and bi-directional horizontal shear deformations with a constant vertical compressive stress. Several types of laminated rubber bearings are used in their experimental studies. They have identified some aspects of bearings, such as hardening and dependence of the restoring forces on the maximum shear strain amplitude experienced in the past. Moreover, some of them also identified coupling effects on the restoring forces of the bearings due to deformation in the two horizontal directions.

Motivated by the experimental results of bearings, different forms of analytical models for bearings are proposed by them. However, their studies are mostly related to illustrating the strain-rate independent mechanical behavior of bearings.

Very few works have been reported in literature regarding the strain-rate dependent behavior of bearings. In this regard, the work of Dall'Asta and Ragni (2006); Hwang et al. (2002) can be reported. They have studied the mechanical behavior of high damping rubber dissipating devices by conducting different experiments, such as sinusoidal loading tests at different frequencies, cyclic shear tests at different strain-rates along with relaxation tests. They have identified the strain-rate dependence of the restoring forces and subsequently developed rate-dependent analytical models. Mullin's softening behavior is also observed in the experiments (Dall'Asta and Ragni, 2006). However, separation of the rate-dependent behavior from other mechanical behavior is not elaborately addressed in their studies.

In this study, an experimental scheme was conducted at room temperature to investigate the rate-dependent mechanical behavior of the laminated rubber bearings under horizontal shear deformation with a constant vertical

compressive load. Three types of specimens with ISO standard geometry, namely HDR, LRB and RB, were used in this scheme. The experimental scheme was comprised of three types of tests: cyclic shear (CS) tests, multi-step relaxation (MSR) tests, and simple relaxation (SR) tests. The CS tests were carried out to identify the instantaneous response, and SR tests were used to identify the viscosity induced rate-dependent behavior and the MSR tests were used to obtain the equilibrium response of the bearings. In addition, a series of sinusoidal loading tests at 0.5 Hz were carried out at different temperatures ranging from 23°C to -30 °C with a view of identifying the basic mechanical characteristics of the bearing at different temperatures, such as the equivalent stiffness and damping of the bearings.

2. EXPERIMENTAL OBSERVATIONS

2.1 Specimens

Three types of bearing specimens, namely high damping rubber bearing (HDR), lead rubber bearing (LRB), and natural rubber bearing (RB) were employed in all experiments. All the specimens had square cross-sectional shape with external in-plane dimensions equal to 250 mm x 250 mm. The reinforcing steel plates had similarly a square planar geometry with external dimensions of 240 mm x 240 mm and thickness of 2.3 mm each. The dimensions and material properties of these specimens are given in Table 1. The dimensions of the test specimens were selected following the ISO standard (ISO, 2005).

2.2 Experimental Set-up and Loading Conditions

The specimens were tested in a computer-controlled servo-hydraulic testing machine at room temperature (23 °C). Displacement controlled tests, under shear deformation with an average constant vertical compressive stress of 6 MPa, were carried out. This mode of deformation is regarded as the most relevant one for application in seismic isolation. The displacement was applied along the top edge of the specimen and the force response was measured with two load cells. All data were recorded using a personal computer. Some of the experimental results are also discussed in somewhere else (Bhuiyan, 2009a; Bhuiyan et al., 2009b).

2.3 Softening Behavior

Virgin rubber exhibits a softening phenomenon, known as Mullins' effect in its first loading cycle. Due to this phenomenon, the first cycle of a stress-strain curve differs

significantly from the subsequent cycles (Mullins, 1969). In order to remove the Mullins softening behavior from other inelastic phenomena, all specimens were preloaded before the actual tests. In the current work, only the specimens of SR and MSR tests were preloaded before the actual tests. The preloading was done by applying 11 cycles of sinusoidal loading at 1.75 shear strain and 0.05 Hz until stable state of the stress-strain response is achieved i.e. that no further softening occurs.

Fig. 1 (a), (b), and (c) present the typical shear stress responses obtained from the pre-loading tests on HDR, RB, and LRB specimens. The same loading history was applied to virgin specimens and preloaded specimens. The time interval between the preloading and the actual test loading was 30 min. The softening behavior in the first loading cycle is evident from the figures for both virgin and preloaded specimens. The Mullins softening effect is not only present in the virgin specimen but also in any preloaded specimens. This implies that Mullins effect can be recovered in quite a very short period owing to the 'healing effect' (Bueche, 1960). As can be seen from the figure, the Mullins effect is more pronounced in HDR than in LRB and RB. All the specimens show a repeatable stress response after passing through 4-5 loading cycles.

2.4 Strain-Rate Dependent Behavior

In the CS test series, a number of constant strain-rate loading tests with a range of 0.05/s to 5.5/s were conducted. Figs. 2 (a), (b), and (c) show the strain-rate dependence of shear stress responses in HDR, RB, and LRB bearings, respectively. For comparison, the equilibrium stress responses are also shown in each figure. The stress responses in the loading path contain three-characteristic features, namely high initial stiffness at low strain levels, followed by large flexibility at moderate strain levels, a large strain hardening at large strain levels. The untangling and/or the separation of weak bonds between filler particles and long chains are associated with reduction of the high initial stiffness. This typical phenomenon is regarded the 'Payne effect' (Lion, 1996).

The final increase of the stiffness is attributed to the limited extensibility of the polymer chains. When compared with the three bearings, the high initial stiffness at a low strain level and the high strain hardening at a high strain level are mostly prominent in HDR at a higher strain rate. However, weaker strain hardening in LRB than that in the other specimens at higher strain levels is also noticeable.

Table 1. Geometry and material properties of the bearings

Specifications	HDR	LRB	RB
Cross section (mm)	240X240		
Number of rubber layers	6		
Thickness of one rubber layer (mm)	5.0		
Thickness of one steel layer (mm)	2.3		
Diameter of lead plug (mm)	--	34.5	--
No. of lead plugs	--	4	--
Nominal shear modulus (MPa)	1.2		

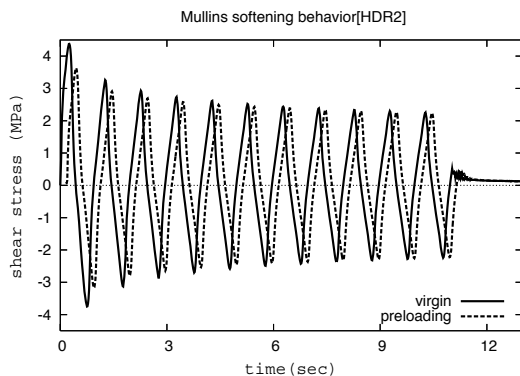
A comparison of hysteresis loops at different strain rates shows that the size of the hysteretic loops increases with increasing the strain rates as shown in Figs.2 (a) to (c). Comparing all the bearings, the HDR demonstrates a larger hysteretic loop than the other bearings. This typical behavior can be attributed that the HDR inherits relatively high viscosity property than the other bearings. Another comparison of the shear stress responses at different strain rates shown in Figs. 2(a) to (c) indicates that the strong strain-rate dependence exists in loading, whereas much weaker strain-rate dependence is observed in unloading.

A further comparison between the loading-path responses at different strain-rates shows that with increasing strain-rate, the stresses increase due to viscosity. At higher strain rates, however, a diminishing trend in increase of stress responses is observed indicating an approach to the instantaneous state. The strain-rate dependence during loading of the bearings is illustrated in Figs.3 (a) to (c).

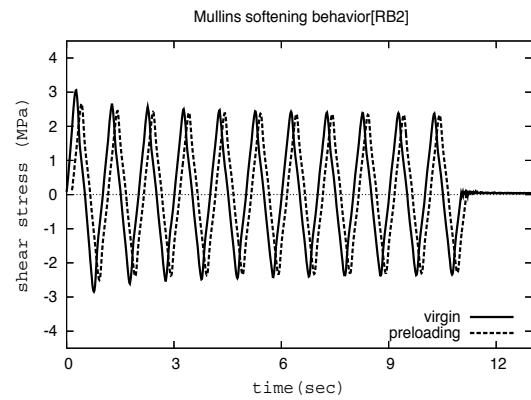
2.5 Viscosity Behavior

The cyclic shear tests presented in the preceding section revealed the existence of viscosity in all the specimens. Simple relaxation (SR) tests were carried out to study the viscosity behavior of the bearings. A series of SR tests at different strain levels were carried out. Figs.4 show the shear stress histories obtained from SR tests conducted at three different shear strain levels of $\gamma = 100, 150,$ and 175% with a strain rate of $5.5/s$ in loading and unloading. The relaxation period after loading and unloading was taken to be 30 min. The stress relaxation histories illustrate the time dependent viscosity behavior of the bearings. For all specimens, a rapid stress relaxation was displayed in the first few minutes; after a while it approached asymptotically towards a converged state of responses.

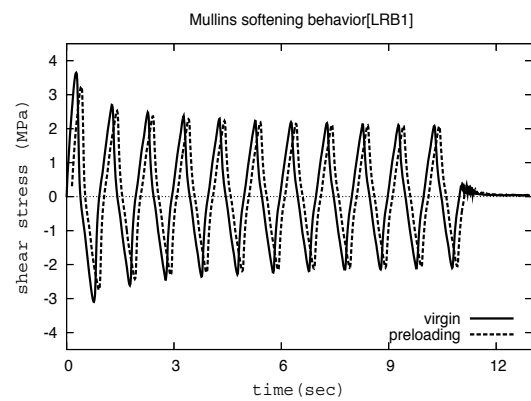
From Figs.4 (a) to (c), HDR shows comparatively high stress relaxation than the other bearings. On the other hand, RB shows much lower stress relaxation than that of other bearings. These observations agree with loading/unloading dependency of rate-dependent behavior observed in the cyclic shear test as illustrated in the preceding section (Figs.2 (a) to (c)). The stress response obtained at the end of the relaxation can be regarded as the equilibrium stress response in asymptotic sense (Lion, 1996).



(a)

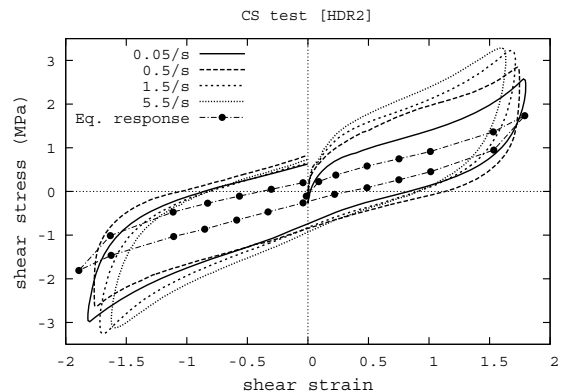


(b)

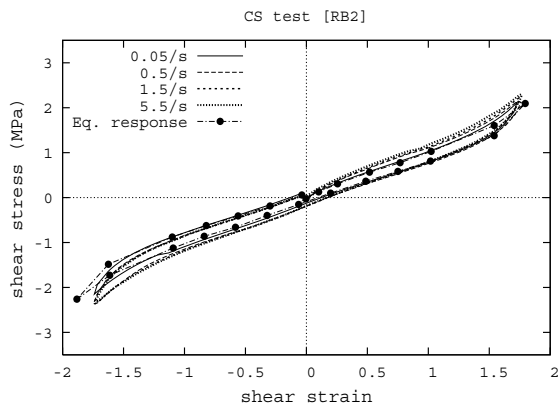


(c)

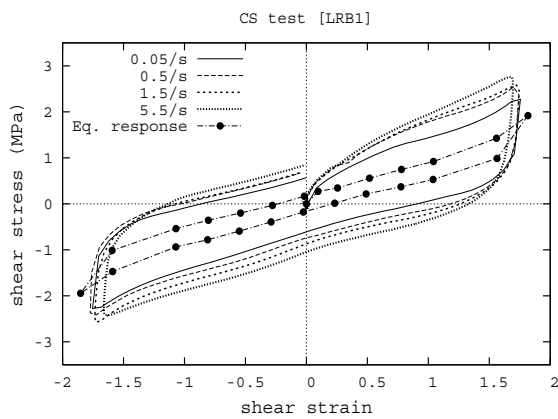
Fig. 1. 11-cycle preloading test on the bearings to remove Mullins effect; (a) HDR, (b) RB, (c) LRB; the legend indicates that the solid line in each figure shows the shear stress histories obtained from the virgin specimens and the dotted line does for the preloading specimens. For clear illustration the shear stress-strain responses are separated by 0.15 sec from each other.



(a)



(b)



(c)

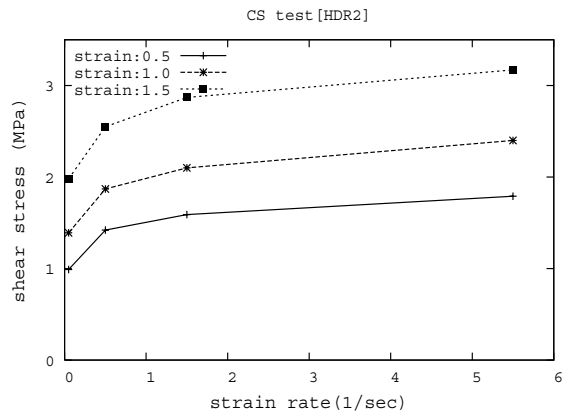
Fig.2. Shear stress-strain relationships obtained from CS tests at different strain rates of the bearings; (a) HDR, (b) RB, (c)LRB; equilibrium response as obtained from MSR tests is also presented for clear comparison.

2.6 Static Equilibrium Hysteresis

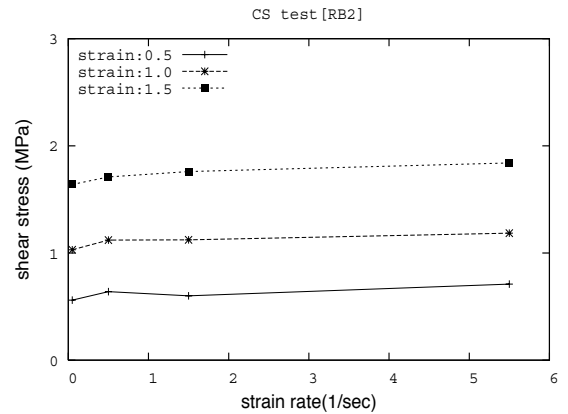
The experimental results obtained from the SR tests at different strain levels showed reduction in stress response during the hold time and approached the asymptotically converged state of responses (i.e equilibrium response). In this context, multi-step relaxation (MSR) tests were carried out to observe the relaxation behavior in loading and unloading paths and to obtain the equilibrium responses (e.g. time-independent response). The shear strain history applied in a MSR test with a maximum shear strain of 1.75 is presented in Fig. 5. In a MSR test, the applied strain is held at several constant strain levels with a relaxation period of 20 min.

Figures 6 to 8 illustrate the shear stress histories and corresponding equilibrium responses obtained in MSR tests of three bearings (HDR, RB, and LRB). At the end of each relaxation period in loading and unloading paths, the stress response converges to an almost constant stress state. The converged stress responses are identified as the equilibrium stresses in an asymptotic sense (Lion, 1996). The shear stress-strain relationships in the equilibrium state can be

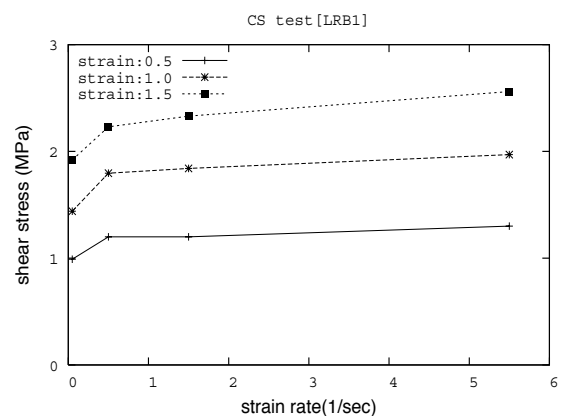
obtained by connecting all the asymptotically converged stress values at each strain level as shown in Figs.6(b) to 8 (b).



(a)



(b)



(c)

Fig.3. Shear stress response as a function of strain rates recorded from CS tests at different strain levels of the bearings; (a) HDR, (b) RB, (c)LRB.

The difference of the stresses between loading and unloading at a particular shear strain level corresponds to the equilibrium hysteresis, which can be easily visualized in the figures. This behavior may be attributed as an irreversible slip process between fillers in the rubber microstructures (Mullins, 1969), which is the resulting phenomenon of breaking of rubber-filler bonds (Bueche, 1960).

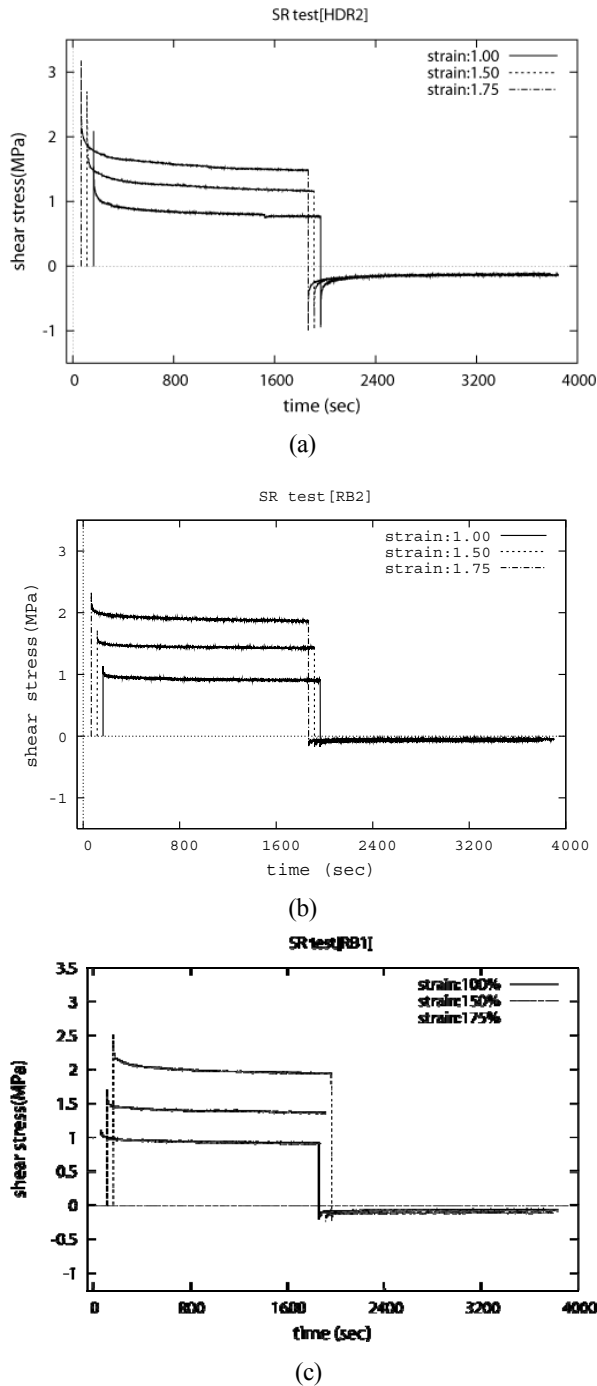


Fig. 4. Shear stress histories obtained from SR tests of the bearings at different strain levels (a) HDR, (b) RB, (c) LRB. For clear illustration, the stress histories have been separated by 50 sec from each other.

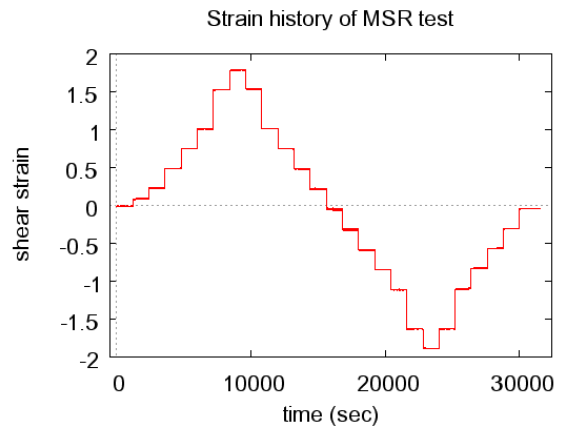


Fig.5. Applied strain histories in MSR test with 1.75 maximum strain level; a shear strain rate of 5.5/s was maintained at each loading and unloading process.

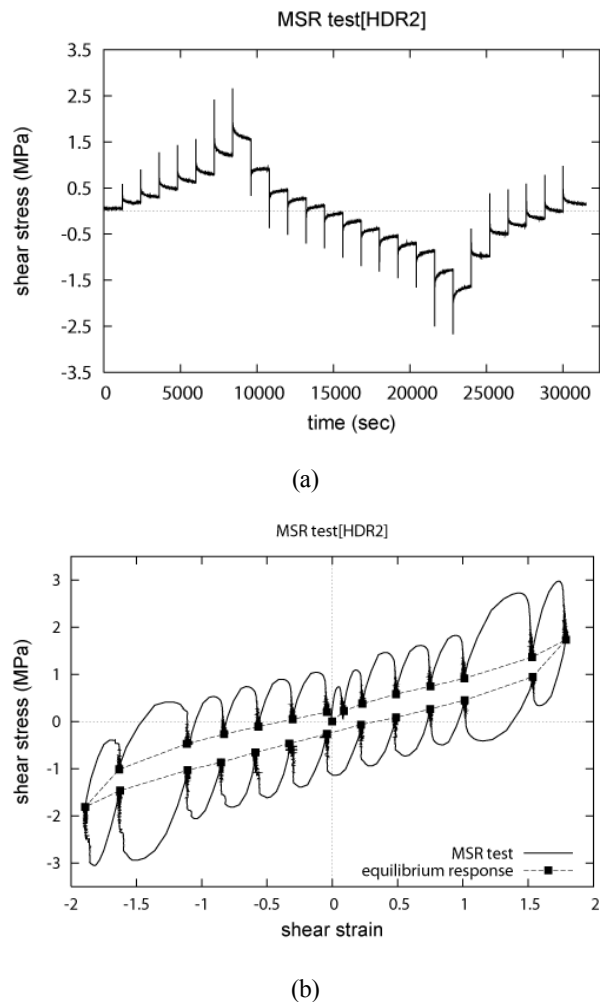
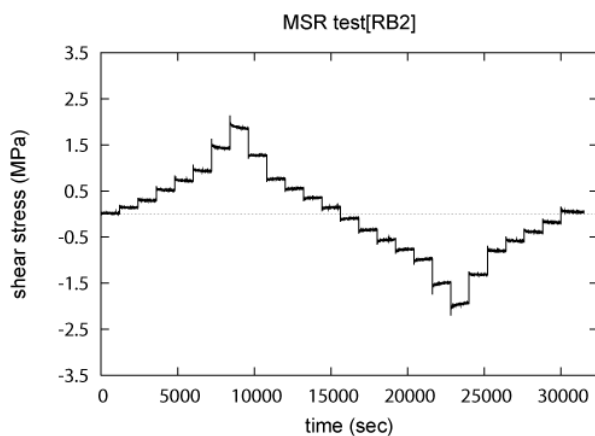
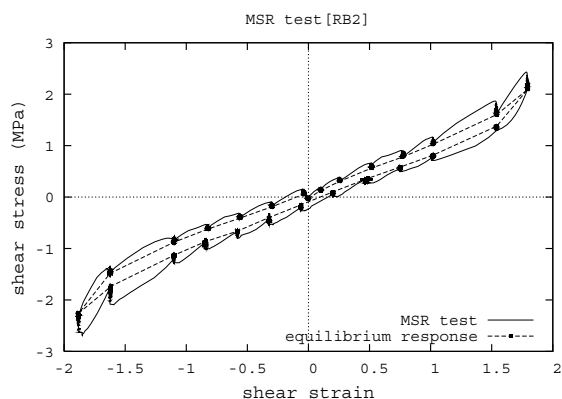


Fig. 6. MSR test results of HDR (a) stress history (b) equilibrium stress response; equilibrium response at a particular strain level shows the response, which is asymptotically obtained from the shear stress histories of MSR test.



(a)



(b)

Fig. 7. MSR test results of RB (a) stress history (b) equilibrium stress response; equilibrium response at a particular strain level shows the response, which is asymptotically obtained from the shear stress histories of MSR test.

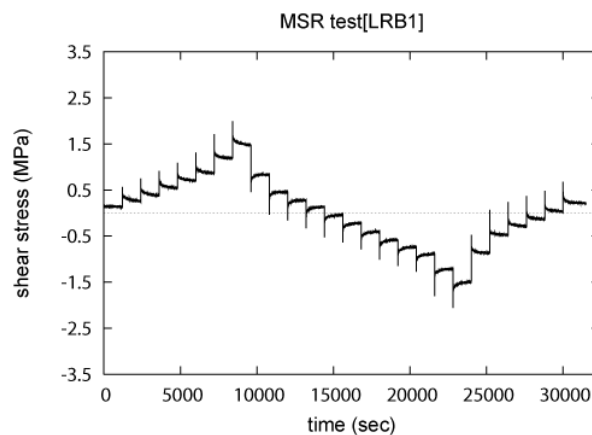
Using the stress history data of Figs. 6 (a) to 8 (a), the overstress can be estimated by subtracting the equilibrium stress response from the current stress response at a particular strain level. Comparing with the overstress for each specimen as shown in Figs.6 (a) to 8 (a), the overstress in loading period is higher than that in unloading at a given strain level. The maximum overstress was observed in HDR, while in RB it was the minimum one.

2.7 Temperature Dependent Behavior

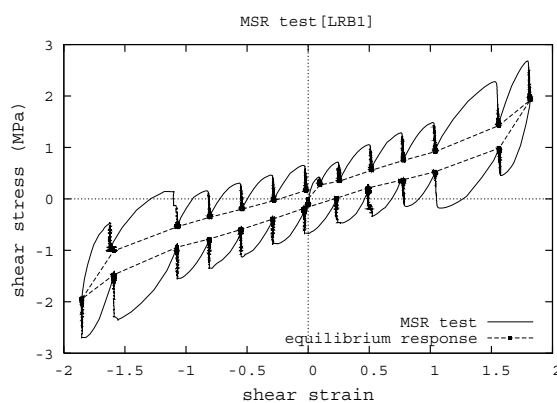
In order to recognize temperature dependent stress-strain responses of the bearings, a series of sinusoidal loading tests of the bearings were carried out at different temperatures ranging from 23°C to -30 °C. The strain amplitude and frequency of the sinusoidal loading were

assigned to 1.75 and 0.5 Hz, respectively. Figs. 9(a), (b), and (c) present the shear stress-strain responses of the HDR, RB, and LRB, respectively. These figures show that the temperature dependence of the stiffness and damping is more significantly appeared in the HDR than that in the other two bearings. Moreover, the trend of increasing the shear stress responses with decrease of temperatures is clearly evident in all the bearings. The equilibrium responses of the bearings as obtained from the MSR test results at 23 °C are also plotted along with the shear stress responses at different temperatures.

Figs. 10 (a) to (c) present the dependency of the equivalent stiffness and equivalent damping constants on temperatures. The ratios of the equivalent stiffness and damping constant at different temperatures to those at 23 °C are plotted. The temperature dependency of the equivalent stiffness is more remarkably emerged in the HDR and RB than LRB, while that of the equivalent damping is more significant in the RB than the others.



(a)



(b)

Fig. 8. MSR test results of LRB (a) stress history (b) equilibrium stress response; equilibrium response at a particular strain level shows the response, which is asymptotically obtained from the shear stress histories of MSR test.

3. CONCLUDING REMARKS

The mechanical tests under horizontal displacement along with a constant vertical compressive load demonstrated the existence of Mullins' effect in all the bearing specimens. However, with the passage of time a recovery of the softening effect was observed. A preloading sequence had been applied before simple relaxation and multi-step relaxation tests were carried out to remove the Mullins' effect.

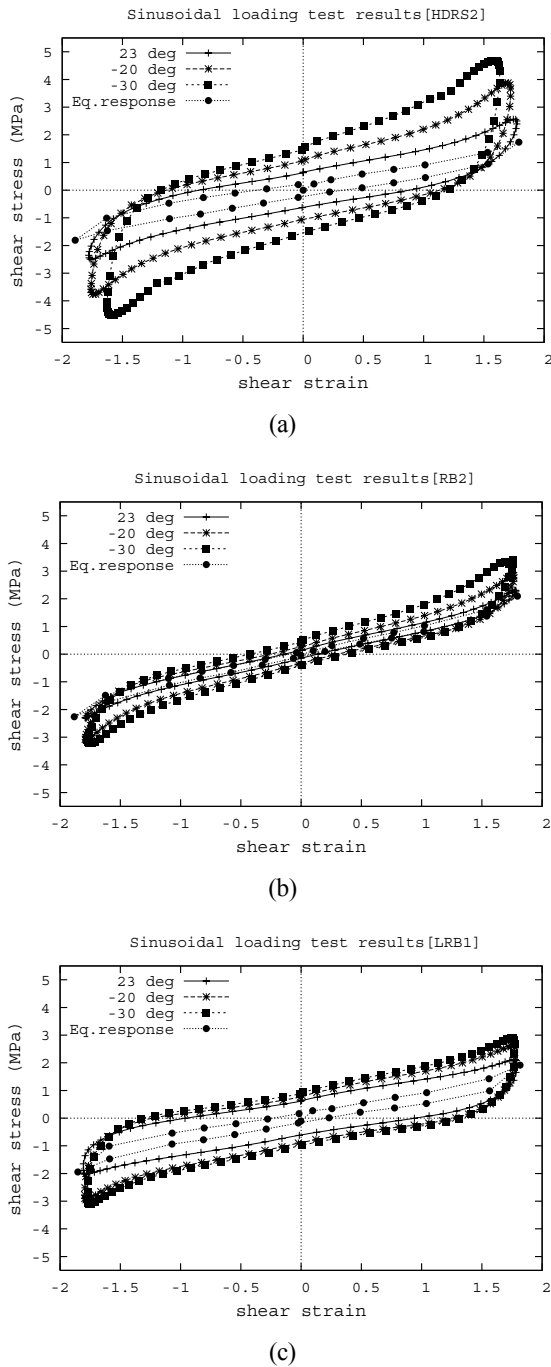


Fig. 9. Sinusoidal excitation test results of the bearings at

different temperatures (a) HDR (b) RB, and (c) LRB. The legend indicates the different temperatures considered in the study.

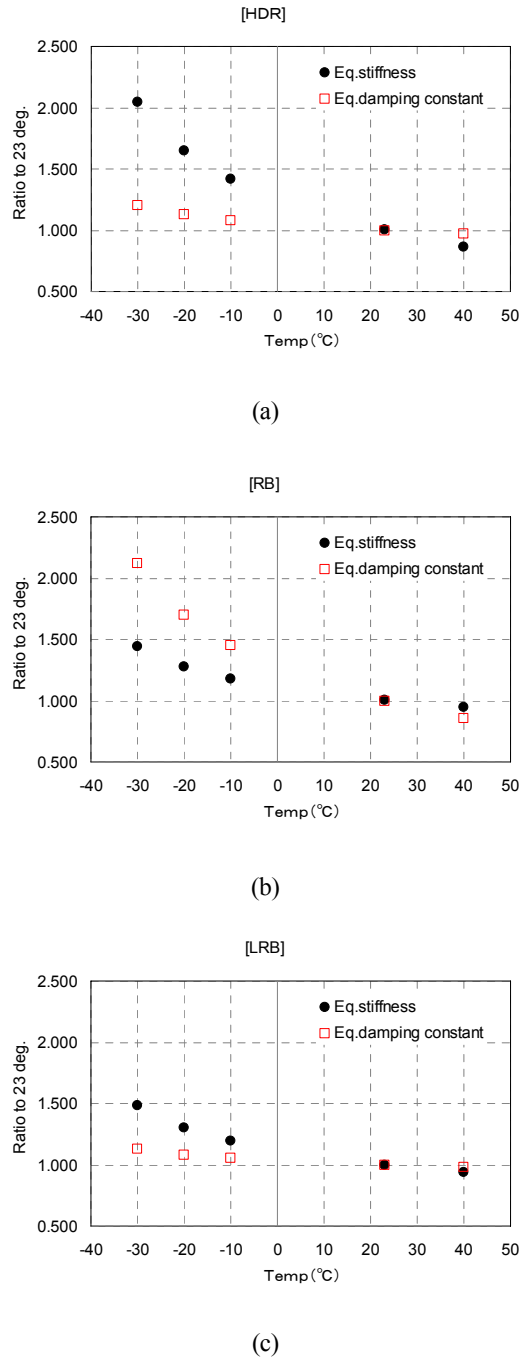


Fig. 10. Temperature dependency of equivalent stiffness and damping constant for (a) HDR (b) RB, and (c) LRB obtained from the sinusoidal loading tests.

Cyclic shear tests at different strain rates illustrated the significant strain-rate dependent hysteresis. The strain-rate dependency in the loading paths was appeared to be stronger

than in the unloading paths. The sinusoidal loading tests at different temperatures showed that the temperature dependence of the stiffness and damping is more significantly appeared in the HDR than the other two bearings. The trend of increasing the shear stress responses with decreasing temperatures is evident in all the bearings.

The simple and multi-step relaxation tests at different strain levels were carried out to investigate the viscosity property in the loading and unloading paths of the bearings. Moreover, in order to identify the equilibrium hysteresis, the multi-step relaxation tests were carried out with different maximum strain levels. When the extent of the strain-rate dependent hysteresis along with other inelastic properties were compared among the three bearings considered in the current study, these effects were found to be more significant in the HDR than the LRB and the RB. More specifically, the strain-rate dependency was more significantly appeared in the HDR than any other bearings. The viscosity property inherited in the HDR might be a possible reason behind the typical behavior of it. On the other hand, the hardening features at high strain levels were found to be more prominent in the RB and HDR than LRB.

Furthermore, temperature dependence on the shear stress-strain responses of the HDR was appeared more significantly than in the LRB and the RB. The experimental observations of the bearings as considered in the current study indicate that a rate-dependent constitutive model is indispensable for describing the mechanical behavior of the bearing.

Acknowledgements

The experimental works were conducted by utilizing the laboratory facilities and bearings-specimens provided by Japan Rubber Bearing Association. The authors indeed gratefully acknowledge the kind cooperation extended by them. The authors also sincerely acknowledge the funding provided by the Japanese Ministry of Education, Science, Sports and Culture (MEXT) in the form of scholarships to carry out this research work

Reference

- Abe, M., Yoshida, J., and Fujino, Y., 2004a. Multiaxial behaviors of laminated rubber bearings and their modeling. I: Experimental study, *Journal of Structural Engineering*, **130**, 1119-1132.
- Aiken, I.D., Kelly, J.M., and Clark, P.W., 1992. *Experimental studies of the mechanical characteristics of three types of seismic isolation bearings*, Proceedings of the 10th World Conference of Earthquake Engineering (WCEE), Madrid, Spain, 2280-2286.
- Bhuiyan, A.R., 2009a. *Rheology modeling of laminated rubber bearings for seismic analysis*, PhD Dissertation, Saitama University, Japan.
- Bhuiyan, A.R., Okui, Y., Mitamura, H. and Imai, T., 2009b. A rheology model of high damping rubber bearings for seismic analysis: identification of nonlinear viscosity, *International Journal of Solids and Structures*, **46**, 1778-1792.
- Bueche, F., 1960. Molecular basis for the Mullins effect. *Journal of Applied Polymer Science*, **4**, 107-114.
- Dall'Asta, A., and Ragni, L., 2006. Experimental tests and

analytical model of high damping rubber dissipating devices, *Engineering Structures*, **28**, 1874-1884.

Hwang, J.S., Wu, J. D., Pan, T, C., and Yang, G, 2002. A mathematical hysteretic model for elastomeric isolation bearings, *Earthquake Engineering and Structural Dynamics*, **31**, 771-789.

International Organization of Standardization (ISO), 2005. *Elastomeric seismic-protection isolators, Part 1: Test methods*, Geneva, Switzerland.

Kikuchi, M., and Aiken, I.D., 1997. An analytical hysteresis model for elastomeric seismic isolation bearings, *Earthquake Engineering and Structural Dynamics*, **26**, 215-231.

Lion, A., 1996. A constitutive model for carbon black filled rubber: Experimental investigations and mathematical representation, *Continuum Mechanics and Thermodynamics*, **8**, 153-169.

Mullins, L., 1969. Softening of rubber by deformation, *Rubber Chemistry and Technology*, **42**, 339-362.

Sano, T., Di and Pasquale, G., 1995. A constitutive model for high damping rubber bearings, *Journal of Pressure Vessel Technology*, **117**, 53-57.